



Full length article

Multi-omics analysis reveals hepatic lipid metabolism profiles and serum lipid biomarkers upon indoor relevant VOC exposure

Gan Miao^{a,1}, Yu Wang^{a,1}, Baoqiang Wang^a, Hongyan Yu^a, Jing Liu^a, Ruonan Pan^a, Chengying Zhou^a, Jie Ning^b, Yuxin Zheng^a, Rong Zhang^{b,*}, Xiaoting Jin^{a,*}

^a Department of Occupational Health and Environmental Health, School of Public Health, Qingdao University, Qingdao, China

^b Department of Toxicology, School of Public Health, Hebei Medical University, Shijiazhuang, China



ARTICLE INFO

Handling Editor: Shoji Nakayama

Keywords:

VOC
Hepatic lipids
Serum biomarkers
Multi-omics
Liver damage

ABSTRACT

As a widespread indoor air pollutant, volatile organic compound (VOC) caused various adverse health effects, especial the damage to liver, which has become a growing public concern. However, the current toxic data are intrinsically restricted in the single or major VOC species. Limited knowledge is available regarding toxic effects, biomarkers and underlying mechanisms of real indoor VOC-caused liver damage. Herein, an indoor relevant VOC exposure model was established to evaluate the hepatic adverse outcomes. Machine learning and multi-omics approaches, including liver lipidomic, serum lipidomic and liver transcriptomic, were utilized to uncover the characteristics of liver damage, serum lipid biomarkers, and involved mechanism stimulated by VOC exposure. The result showed that indoor relevant VOC led to the abnormal hepatic lipid metabolism, mainly manifested as a decrease in triacylglycerol (TG) and its precursor substance diacylglycerol (DG), which could be contributed to the occurrence of hepatic adverse outcomes. In terms of serum lipid biomarkers, five lipid biomarkers in serum were uncovered using machine learning to reflect the hepatic lipid disorders induced by VOC. Multi-omics approaches revealed that the upregulated *Dgkq* disturbed the interconversion of DG and phosphatidic acid (PA), leading to a TG downregulation. The in-depth analysis revealed that VOC down-regulated FoxO transcription factor, contributing to the upregulation of *Dgkq*. Hence, this study can provide valuable insights into the understanding of liver damage caused by indoor relevant VOC exposure model VOC exposure, from the perspective of multi-omics analysis.

1. Introduction

Ambient air pollution exhibited increasingly serious hazard to global public health in recent years, posing a significant impact on premature mortality and morbidity (Fuller et al., 2022). According to the Global Burden of Disease (GBD) study in 2015, 4.2 million deaths were linked to ambient air pollutants, while an additional 2.8 million deaths were caused by household air pollution (Cohen et al., 2017). Moreover, people spend approximately 90 % of their time indoors, thus more likely suffering from indoor air pollution exposure (Cohen et al., 2017). Yet in recent years, the health risks of indoor air pollution on human were largely neglected, with focused primarily on the impact of outdoor air pollution. It is noteworthy that volatile organic compound (VOC) played increasingly significant role in indoor environment, for their capacity to react with other pollutants present indoors to produce harmful

secondary pollutants (Cohen et al., 2017). Exposure to VOC have demonstrated to be intimately relevant to various adverse health effects, including allergies, respiratory diseases, liver dysfunction, and cancer (Shuai et al., 2018; Villeneuve et al., 2013).

Liver acts as a pivotal organ for the regulation of metabolic pathways, detoxification of hazardous substances originating from the external environment, and purification of the blood (Stange et al., 2000). Epidemiological studies have confirmed the relationship between chronic exposure to organic solvents and liver damage, such as cholestasis, in industrial workers (Liu et al., 2009). Moreover, VOC mixture (formaldehyde, benzene, toluene, and xylene) exposure also induced significant DNA damage and oxidative damage in the liver (Wang et al., 2013). Despite epidemiologic studies suggesting the strong association between VOC exposure and liver hazards, the characteristicly adverse outcome of liver injury induced by VOC and underlying

* Corresponding authors.

E-mail addresses: rongzhang@hebmu.edu.cn (R. Zhang), xtjin@qdu.edu.cn (X. Jin).

¹ Contributed equally.

mechanisms remain poorly understood.

Liver lipid homeostasis can exert crucial influence on coordinating fatty acid uptake, synthesis and oxidative decomposition, lipid export and redistribution of liver (Fang et al., 2022). Hepatic lipid disorder is clinically relevant to various disease, such as obesity, type 2 diabetes, liver fibrosis and even primary liver cancer (Carotti et al., 2020; Fang et al., 2022). For instance, due to the increased hepatic uptake and de novo lipogenesis, a compensatory enhancement of fatty acid oxidation is insufficient in normalizing lipid levels in non-alcoholic fatty liver disease (NAFLD) (Fang et al., 2022). Previous study focused on the assessment of single or mixed component of VOC on liver lipid metabolism. For example, chloroethanol, one metabolite of VOC, altered lipid metabolism and resulted in hepatic steatosis due to changes in white adipose tissue lipolysis (Yu et al., 2022). Whether indoor relevant VOC could perturb the homeostasis of lipid metabolic profiles in the liver, considering as the indicators for liver injury, remained to be elucidated.

Biomarkers in blood can estimate the impact of environmental pollutants on human health for the capacity to reflect the internal conditions of organisms (Wallace et al., 2016). Due to synchronous alternations between serum lipid response and abnormal liver lipid levels, the upregulation or downregulation of serum lipid is considered as a “warning” of the adverse outcome of liver (de Mello et al., 2012; Konieczna et al., 2014). For instance, serum TG and cholesterol (TC) were investigated to evaluate liver damage and lipid metabolism disorder induced by exterior compounds (Yu et al., 2022). Previous study merely demonstrated that the upregulation of serum TG and TC was accompanied by decreased liver function in biochemical workers with long-term occupational VOC exposure (Salehpour et al., 2019). Limited knowledge is available regarding serum lipid biomarkers reflecting the alteration of hepatic lipid metabolism profiles caused by indoor environmental VOC exposure.

Multi-omics combination technology is capable of improving the sensitivity and accuracy of assessment for the characteristics of liver damage, and revealing the interaction between environmental exposure and organisms (Da et al., 2020; Wang et al., 2021). In the current study, combined with multi-omics combination technology (liver lipidomic, serum lipidomic, and liver transcriptomic), an indoor relevant VOC combined exposure mouse model was established to evaluate the adverse effects on hepatic lipid, identify serum lipid biomarkers reflecting disorder of hepatic lipid, and clarify the mechanism of liver injury upon VOC exposure. These findings provide valuable insights into the understanding of liver damage caused by indoor VOC exposure and potential interventions to mitigate its adverse effect.

2. Materials and methods

2.1. Animal experiment and VOC exposure

Six-week-old male C57BL/6J mice (22.2 ± 1.1 g), obtained from the Vital River Laboratories (Beijing, China), were housed in a standard animal centre of Hebei Medical University (23 °C, 12-hour light–dark cycle). All mice were maintained on a standard pellet diet and provided with free access to distilled water for drinking. After acclimatization for 1 week (W), mice were randomly divided into control (CON) group and VOC group with 20 mice in each group. As described in our previous study (Zheng et al., 2022), mice were exposed with or without filtered VOC exhaust from the volatilisation of decorative paints (Shijiazhuang paint factory, Shijiazhuang, China) for 8 h (h) per day. The exposure was continuously performed for 4 W and 8 W, respectively. We adopted separate cage exposure equipment in this study to simulate the indoor relevant VOC environment. The indoor air was pumped by a blower, filtered by filter membranes, and sent to the mouse cage. Mice in the CON group inhaled room air filtered through a high efficiency particulate air (HEPA) and activated carbon (AST, environmental science & technology Co., Ltd, China) to remove particulate matter and VOC,

respectively. Meanwhile, mice in the VOC group inhaled air filtered through HEPA to remove particulate matter. The sustained exposure concentration is maintained through stable internal environmental conditions within the unit, including a constant temperature of 25 °C, relative humidity of 50 %, and a pressure difference of 25 kPa. The mean daily concentrations of VOC in the CON and VOC rooms were 333.64 ± 82.57 ppbv and 613.86 ± 160.13 ppbv, respectively (Table S1). Furthermore, the concentration of each VOC component was measured at the 8th W of exposure, which was presented in Table S2. All experimental procedures for this research were approved by the Institutional Animal Care and Use Committee of Hebei Medical University, and performed under the institutional guidelines for ethical animal usage. All mice were euthanized with pentobarbital sodium treatment immediately following the last exposure. Liver and plasma in mice were collected for the subsequent lipidomic and transcriptomic assay.

2.2. Hematoxylin-eosin staining

Liver tissue samples from CON and VOC groups were fixed in 4 % paraformaldehyde (PFA) for 24 h and subsequently embedded in paraffin. Liver tissue section with 5 μ m thickness was then submitted to the hematoxylin-eosin (H&E) staining procedure, which was carried out as previously described (Zhang et al., 2020). Stained sections were observed using a light microscopy (OlympusBX59, Japan) for the evaluation of histological alteration. After imaging, the area and perimeter of central vein in each section were measured using the Image Pro Plus software (version of 6.0). Furthermore, the number of inflammatory foci in randomly selected representative sections was counted to assess the degree of liver inflammation. Briefly, a total of 6 sections were analyzed. For each section, 6 high-power fields (HPFs) were randomly selected and the number of inflammatory foci within each HPF was counted. To ensure consistency, two independent observers blinded to the experimental conditions counted the foci in each section. Any discrepancies between the observers were resolved through consensus.

2.3. Oil red O staining

The 4 % PFA fixed liver samples were frozen in optimal cutting temperature (OCT) compound, and sliced into 15 μ m thick sections. Neutral lipids of all sections were stained using oil red O (Servicebio, China), followed by the observation and photograph with the Nikon Eclipse E100 microscope and Nikon DS-U3 imaging system (Nikon, Japan). Three fields of view from each liver section were randomly selected. In each field of view, the percentage of positive oil red O staining area was calculated using the ImageJ color thresholding tool of ImageJ software (version of 1.80), and the average percentage was calculated for each liver section.

2.4. Lipidomic assay

The liver and serum samples from CON and VOC groups were submitted to the lipidomic analysis. Briefly, liver tissue was homogenized in a chloroform–methanol mixed solution (2:1, –20 °C) using a tissue grinder (BE-2600, Kylin-Bell, China). Serum samples were vortexed in a chloroform–methanol mixture. The obtained extracts were mixed with deionized water, and separated by centrifugation (12,000 g, 5 min) to obtain the lower layer fluid into a new tube. After drying down in vacuum, the extracts were reconstituted in isopropanol, and filtered through a 0.22 μ m membrane for the subsequent liquid chromatography-mass spectrometry (LC-MS) analysis. The QC samples for liver or serum, a pool of samples ($n = 8$), were mixed from 20 μ L of each liver or serum sample. To ensure sample accuracy, the QC samples were interspersed during the sampling injection process, and five biological replicates were performed for each group.

LC-MS assay was conducted under the help of BioNovoGene Technology Co., Ltd. (China). In brief, samples were analyzed in electrospray

ionization (ESI) mode with a liquid chromatography instrument (Vanquish, Thermo Fisher, USA) combined with a mass spectrometer (QE Focus, Thermo Fisher, USA). The separation of lipid was achieved using an ACQUITY UPLC® BEH C18 (100 × 2.1 mm, 1.7 μm, Waters, USA) at a column temperature of 55 °C. The mobile phase was consisted of acetonitrile: water 60:40 (0.1 % formic acid + 10 mM ammonium formate) (solvent A) and isopropanol: acetonitrile 90:10 (0.1 % formic acid + 10 mM ammonium formate) (solvent B). The gradient elution was as follows: 0–5 min, 70–57 % A; 5–5.1 min, 57 %–50 % A; 5.1–14 min, 50 %–30 % A; 14–14.1 min, 30 % A; 14.1–21 min, 30 %–1 % A; 21–24 min, 1 % A; 24–24.1 min, 1 %–70 % A; 24.1–28 min, 70 % A. The injection volume was 2 μL.

Acquired data were analyzed using the LipidSearch software. Lipid species were identified based on their accurate mass and retention time. The peak areas of identified lipid species were normalized to the internal standard and then used for the subsequent statistical analysis. Relative abundance of each lipid species was calculated as a percentage of the total ion intensity in the sample. Finally, Variable importance in projection (VIP) values and one-way ANOVA *p*-values were combined after statistical analysis to identify the significantly different lipid profiles between CON and VOC groups.

2.5. Machine learning analysis of liver lipidomic and serum lipidomic

The least absolute shrinkage selection operator (LASSO) method based on the R package “glmnet” was employed to perform high-dimensional data regression for the dual lipidomics, including liver lipidomic and serum lipidomic. The most effective predictors were selected, and the lambda value was set to one standard error during the LASSO regression process. Obtained biomarkers were evaluated by calculating the area under the curve (AUC) values using the R package “pROC”. Canonical correspondence analysis (CCA), used by the R package “vegan”, a widely used multivariate gradient analysis in omics studies, was utilized to determine the correlation between the abundance of serum lipid biomarkers and hepatic lipid. The correlations between individual serum lipid biomarkers and hepatic lipid were analyzed using the Pearson correlation analysis with the “corrplot” R package.

2.6. Transcriptomic assay

RNA-sequencing (RNA-seq) and gene expression analysis were performed under the help of BioNovoGene Technology Co., Ltd. (Suzhou, China). Total RNA was first extracted from liver samples using a Trizol (YEASEN, China) according to the manufacturer’s instructions. RNA concentration and purity were determined by measuring the absorbance at 260 and 280 nm using a NanoDrop 2000 spectrophotometer (Thermo Fisher, USA). RNA quality and effective concentration were assessed using an Agilent 2100 Bioanalyzer (Agilent, USA). After RNA extraction, purification, and library building, next generation sequencing (NGS) with paired-end (PE) was used for sequencing on the Illumina platform.

The RNA-Seq data was processed and analyzed. In brief, the raw data was filtered by Cutadapt, quality-checked by FastQC, and aligned to the reference genome with Tophat2. Gene expression quantification was presented using HTSeq and expressed in fragments per kilobase of exon per million reads mapped (FPKM). Differential expression analysis was performed using the R package “DESeq2,” with differential expression genes (DEGs) identified using specific thresholds: \log_2 (fold change) > 1, *p* < 0.05. Functional and pathway enrichment analysis of DEGs was performed using R packages “clusterProfiler”, “org.Mm.eg.db” and “enrichplot”.

2.7. Combinatorial analysis of transcriptomic and lipidomic data

Pearson correlation analysis was executed by utilizing the “corrplot” R package, and the network graph was drawn based on the “igraph” R

package. The strongly correlative lipids and genes were correlated with the kyoto encyclopedia of genes and genomes (KEGG) using MetaboAnalyst (version of 3.0), a web application that utilizes KEGG metabolic pathways as a pathway knowledge base. Perturbed metabolites were ranked according to their statistical likelihood of being found greater than chance (*p* < 0.05), with corrections made for multiple comparisons. Potential impact of these metabolites on pathways was analyzed according to their position and topology.

2.8. Immunofluorescence assay

The paraffin-embedded lung tissues were cut into 4 μm thick slices, followed by de-paraffinization, re-hydration, antigen retrieval, and serum sealing. The slices were incubated with DAGK (1:100, Affinity Biosciences, China) or FOXO1 (1:100, Zenbio, China) primary antibody at 4 °C overnight, followed by the incubation of fluorescent goat anti-rabbit IgG (H + L) secondary antibody (Boster, China) for 45 min. Then the nucleus was counterstained with 4',6-diamidino-2-phenylindole (DAPI; Boster, China). After sealing with anti-fluorescence quenching sealing tablets, the slides were mounted in gelvatol for confocal immunofluorescence analysis, and then photographed under a fluorescence microscope (Olympus, Japan).

2.9. qPCR analysis

The total RNA of mice liver was extracted using Trizol (YEASEN, China). Then, 500 ng of total RNA was transcribed to cDNA using a reverse transcription kit (Sparkjade, China) in an ABI Proflex™ Thermal cycler (Thermo Fisher, USA). The cDNA was then subjected to qPCR using a 2 × SYBR qPCR mix (Sparkjade, China) and the QuantStudio™ 7 Flex Real-Time PCR instrument (Thermo Fisher, USA). The reaction was performed in a total volume of 10 μL, consisting of 0.4 μL primers, 2 μL cDNA, 2.4 μL RNase free H₂O, and 0.2 μL ROX reference dye. The β-actin of reference gene was used for normalization, and detailed primer pairs were shown in Table S3 (Supplementary file).

2.10. Statistical analysis

Except for the data of transcriptomic and lipidomic, the results of each group were presented as mean ± standard error of the mean (SEM) with at least three biological replicates. Data analyses were performed using GraphPad Prism (version of 9.1.0), R (version of 4.2.1) and RStudio (version of 2023.03.0 + 386). Student’s *t*-tests were conducted to compare the two groups. Significant differences were considered in all tests when *p* was < 0.05.

3. Results

3.1. Characteristics of liver lipid metabolism in mice upon VOC exposure

To investigate the disturbance characteristics of indoor relevant VOC on hepatic lipid, a whole-body inhaled VOC mouse exposure model was established. Liver tissue was collected at two exposure time points, i.e. 4 W and 8 W, which was capable of simulating the indoor relevant VOC exposure (Fig. 1A). Both body weight and liver coefficient of mice showed no significant alteration upon VOC exposure for 4 W and 8 W (Fig. S1 and S2). The quality control (QC) samples of lipidomic analysis indicated the reliability of results (Fig. S3). PCA analysis showed clear differentiation in lipid composition between the CON and VOC groups, and a total of 20 lipid subclasses were identified, with glycerides, glycerophospholipids, glycolipids, and sphingolipids being predominant (Fig. S4). As illustrated in Fig. 1B, VOC exposure at 4 W and 8 W resulted in a significant decrease in glycerides, including TG, DG and mono-glyceride (MG). For the glycerophospholipids, phosphatidylglycerol (PG) and lysophosphatidyl-ethanolamine (LPE) decreased, while PA and phosphatidylcholine (PC) increased. Partial glycolipid (MGDG) and

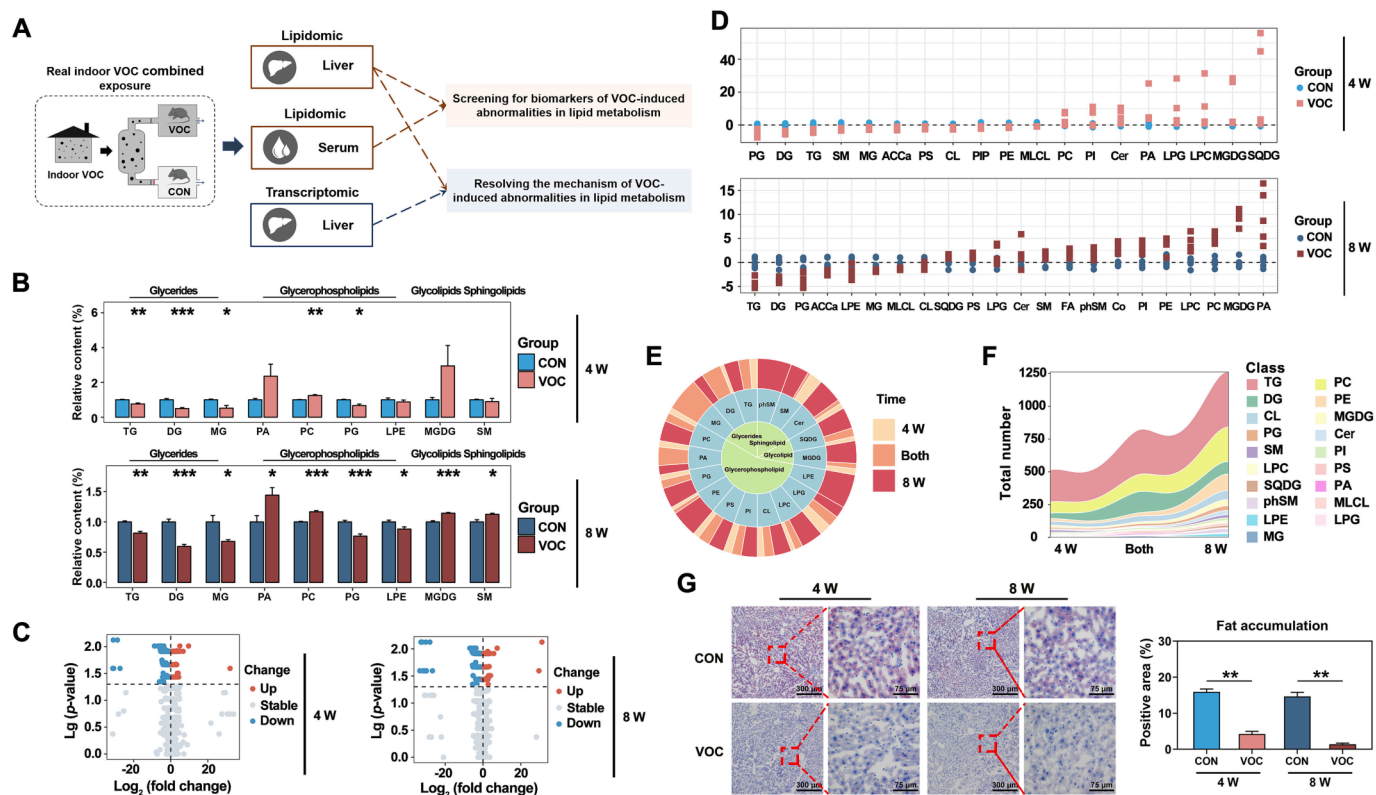


Fig. 1. Characteristics of hepatic lipids in mice upon indoor relevant VOC exposure. (A) Schematic showing experimental design for animal experiments. (B) Relative lipids content changes (% total lipids) in CON and VOC mice. (C) Volcano plot of differential lipids in VOC group compare with CON group at 4 W and 8 W. (D) Z-score of differential lipid species in CON and VOC mice. Each dot represents a single sample. (E) Pie chart of the time distribution of differential lipids across individual lipid categories. (F) The stacking of different lipid quantities in different lipids at different time points. (G) Representative images and quantitative data of oil red O staining in mice liver. Scale bar = 75 μ m. Data were expressed as mean \pm SEM. * p < 0.05, ** p < 0.01, *** p < 0.001, versus the respective CON group.

partial sphingolipid (SM) increased significantly only in 8 W of VOC exposure. No significant alterations were observed in other lipid subclasses (Fig. S5).

To further address the targeting characteristics of VOC on hepatic lipids, differentially expressed lipids (DELS) were screened at thresholds of variable importance value (VIP > 1.0) and p value (p < 0.05). Compared to the CON group, 718 DELS were detected after 4 W of VOC exposure, while 1255 DELS were found after 8 W (Fig. 1C). At the subtype level of all major lipid classes, TG, DG, PG, PA, and PC showed the most significant changes (Fig. S6). As shown in Fig. 1D, 4 W of VOC exposure decreased all three glycerides (TG, DG, and MG), but increased the direct metabolites of DG such as PA and PC, indicating that VOC exposure led to lipid metabolism disorder in the liver. These changes were more pronounced at 8 W, with TG showing the greatest decrease and PA exhibiting the most significant increase among all lipid categories, suggesting that VOC exposure may cause a tended conversion of DG to PA. Clustering heatmaps of the DELS showed that after 4 and 8 weeks of exposure, the DELS split into two large clusters of either increased or decreased (Fig. S7). The DELS of ceramide (Cer) and lysophosphatidylcholine (LPC) were predominantly in the increased clusters after 4 weeks of exposure, and the DELS of Cer were virtually unchanged at 8 weeks relative to 4 weeks but more DELS for LPC appeared in the increased clusters.

To examine the temporal response of hepatic lipids to VOC exposure, DELS at various time points were further analyzed. 448 lipids responded to VOC exposure at both 4 and 8 W, while 270 lipids responded exclusively to 4 W and 807 lipids responded only to 8 W (Fig. S8). DELS were further categorized across lipid subclasses. As illustrated in Fig. 1E and F, glycerides, particularly MG and DG, showed significant responses at both 4 and 8 W, while glycerophospholipids, glycolipids, and sphingolipids primarily responded at 8 W. Furthermore, the number of DEL

species was higher at 8 W, with TG, DG, PC, PE, and cardiolipin (CL) being the most sensitive lipid categories to VOC exposure, suggesting that 8 W was the main time period for VOC to disturb the liver lipid metabolism.

Oil red O staining confirmed the lipid disorder observed in lipidomic, revealing lighter staining of lipid droplets in VOC-exposed liver after 4 and 8 W. Quantitative analysis showed a significant reduction in neutral fat content (Fig. 1G), indicating impaired fat accumulation. HE staining indicated no significant alterations in the central vein area but showed increased inflammatory foci and decreased hepatic sinusoid width after 8 W of VOC exposure (Fig. S9). The above results revealed that indoor VOC can lead to abnormal liver lipid metabolism, mainly manifested by the decrease of TG and its precursor DG, accompanied by the occurrence of hepatic adverse outcomes.

3.2. Identification of serum lipid biomarkers reflecting abnormal hepatic lipids by VOC exposure

To identify the serum lipid biomarkers reflecting disorder of hepatic lipids by 8 W of VOC exposure, serum lipidomic analysis was then performed. The PCA plot showed a clear distinction between the CON group and VOC group, indicating a significant alteration of serum lipid profiles (Fig. 2A). There was no significant change in the content of total lipids in serum after 8 W of VOC exposure (Fig. S10). Among the glycerides, glycerophospholipids, sphingolipids, and glycolipids, the relative levels of serum TG decreased and LPC increased under 8 W of VOC exposure (Fig. 2B-E), which were in accordance with the alterations in the liver. Volcano plots were further used to screen for DELS in serum, and 214 DELS were identified in the VOC and CON groups, including 118 up-regulated DELS and 96 down-regulated DELS upon VOC exposure (Fig. 2F). Among the differential lipids in serum, glycerides such as TG

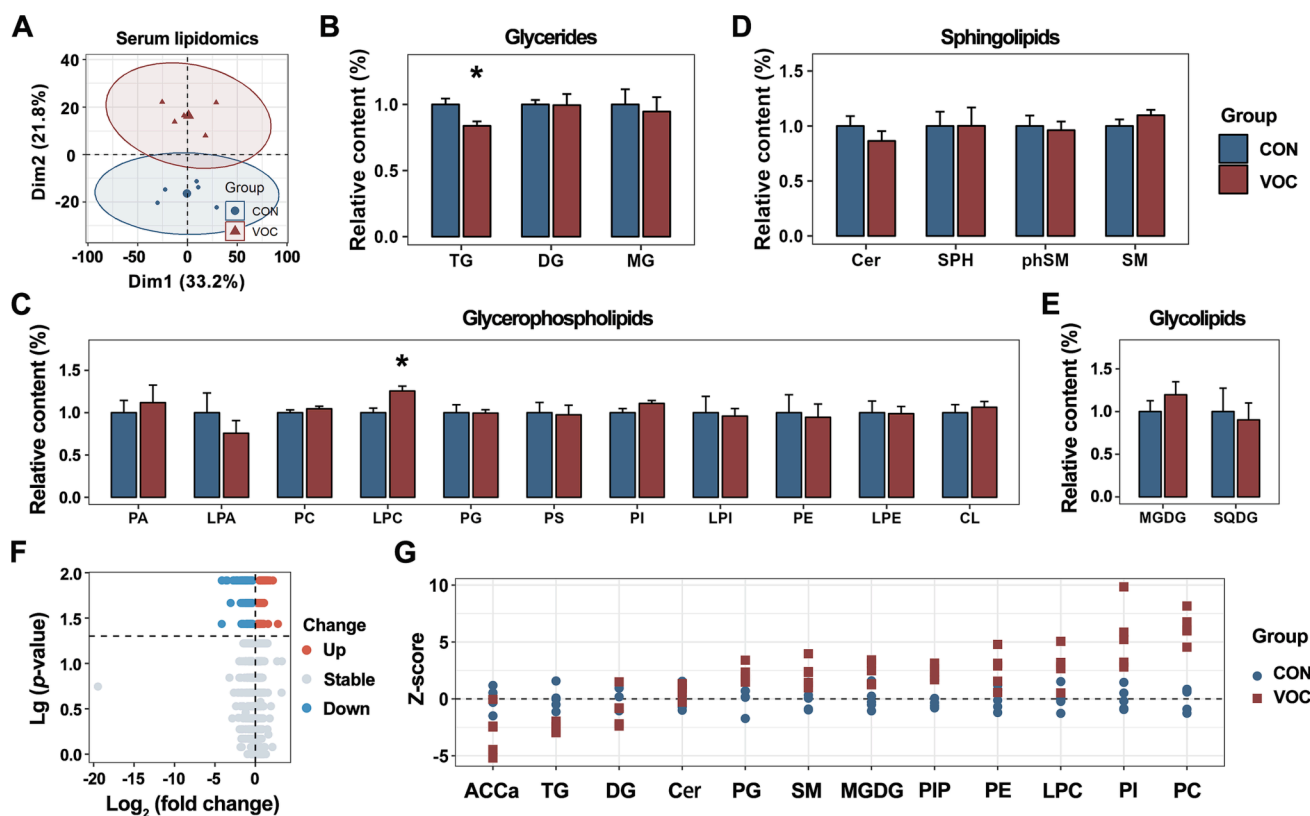


Fig. 2. Effects of VOC exposure for 8 W on serum lipids. (A) The differences in global lipid profiles between CON and VOC groups. Relative (B) glycerides, (C) glycerophospholipids, (D) sphingolipids, and (E) glycolipids content changes (% total lipids) in CON and VOC mice. (F) Volcano plot for individual lipids in CON and VOC groups, comparing the fold change and p value. (G) Differential lipid species in CON and VOC groups. Each dot represents a single sample. Data were expressed as mean \pm SEM ($n = 5$). * $p < 0.05$, versus the respective CON group.

and its precursor lipid DG decreased in the VOC-exposed group, and the content of glycerophospholipids (downstream of DG) such as PC, PE and LPC increased (Fig. 2G). These data demonstrated that 8 W of VOC exposure decreased the overall serum TG levels and DELs of glycerides, but increased the downstream glycerophospholipids, suggesting an increase in the direct conversion of glycerides to glycerophospholipids.

The dual lipidomics data from liver and serum were subsequently analyzed to identify potential serum lipid biomarkers for the hepatic lipid alteration stimulated by 8 W of VOC exposure. Considering the decreased TG levels in both liver and serum, the potential correlation was firstly determined. Pearson correlation analysis in Fig. 3A found that serum TG positively correlated with liver TG ($r = 0.66$, $p = 0.04$), thus TG was concentrated to screen the potential lipid biomarkers. The model incorporated all the DELs of TG in serum lipids as characteristic variables and the proportion of TG in liver lipids as outcome variables. Based on ten-fold cross-validation, it was determined that the LASSO logistic regression model at $\log(\lambda) = 18.241$ had the smallest binary deviance (Fig. 3B). Five lipid biomarkers were further identified using the LASSO logistic regression model (Fig. 3C), including TG (16:0_16:1_18:3), TG (16:1_16:1_18:3), TG (20:1_22:6_22:6), TG (22:4_18:2_18:2), and TG (51:6) (Table S4). The five biomarkers reflected hepatic lipid disturbances dominated by decreased TG.

To further examine the accuracy of the above five biomarkers reflecting disorder of hepatic lipid caused by VOC, adjusted receiver operating characteristic (ROC) curves were calculated for each of the biomarkers. As illustrated in Fig. 3D, the area under the ROC curve (AUC) for each biomarker was 1, 1, 0.92, 0.96, and 0.88, respectively, while the AUC for combining the five biomarkers was 0.96, indicating that these biomarkers are highly accurate for determining VOC exposure. A discriminant model of canonical correlation analysis (CCA) was also employed to verify whether the combination of five biomarkers can

distinguish the VOC-exposed group from the CON group. As shown in Fig. 3E, the combination of these biomarkers revealed a significant correlation with the levels of several significantly altered lipid classes (i. e., DG, LPE, PC, PG, TG) in the liver in VOC group. Moreover, these biomarkers employed alone also showed significant correlations with several liver lipid classes affected by VOC (Fig. 3F), indicating that these markers can well reflect the changes in hepatic lipid metabolism. Combining these results, TG (16:0_16:1_18:3), TG (16:1_16:1_18:3), TG (20:1_22:6_22:6), TG (22:4_18:2_18:2), and TG (51:6) in serum were identified as lipid biomarkers for the supervision of abnormal hepatic lipid caused by VOC exposure.

3.3. Potential mechanism of abnormal hepatic lipid metabolism in mice upon VOC exposure

To track the potential mechanism of disturbed liver lipid metabolism of mice following 8 W of VOC exposure, transcriptional analysis was performed on the same liver samples. PCA revealed significant differences between CON and VOC groups (Fig. 4A). Gene set enrichment analysis (GSEA) was then used to examine changes in relevant metabolic pathways involved in glycerolipids and glycerophospholipids, the main types of hepatic lipid disorders. As illustrated in Fig. 4B and C, both glycerolipid metabolic pathway and glycerophospholipid metabolic pathway were downregulated by VOC, suggesting that the decrease in glycerolipids was not only dependent on the direct degradation but also the interconversion with glycerophospholipids.

To further gain insight into the interconversion between glycerolipids and glycerophospholipids, the expression of genes involved in the glycerides and glycerophospholipids metabolic pathways was investigated in both CON and VOC groups. The gene expressions of these enzymes involved in metabolism were altered by VOC exposure, with

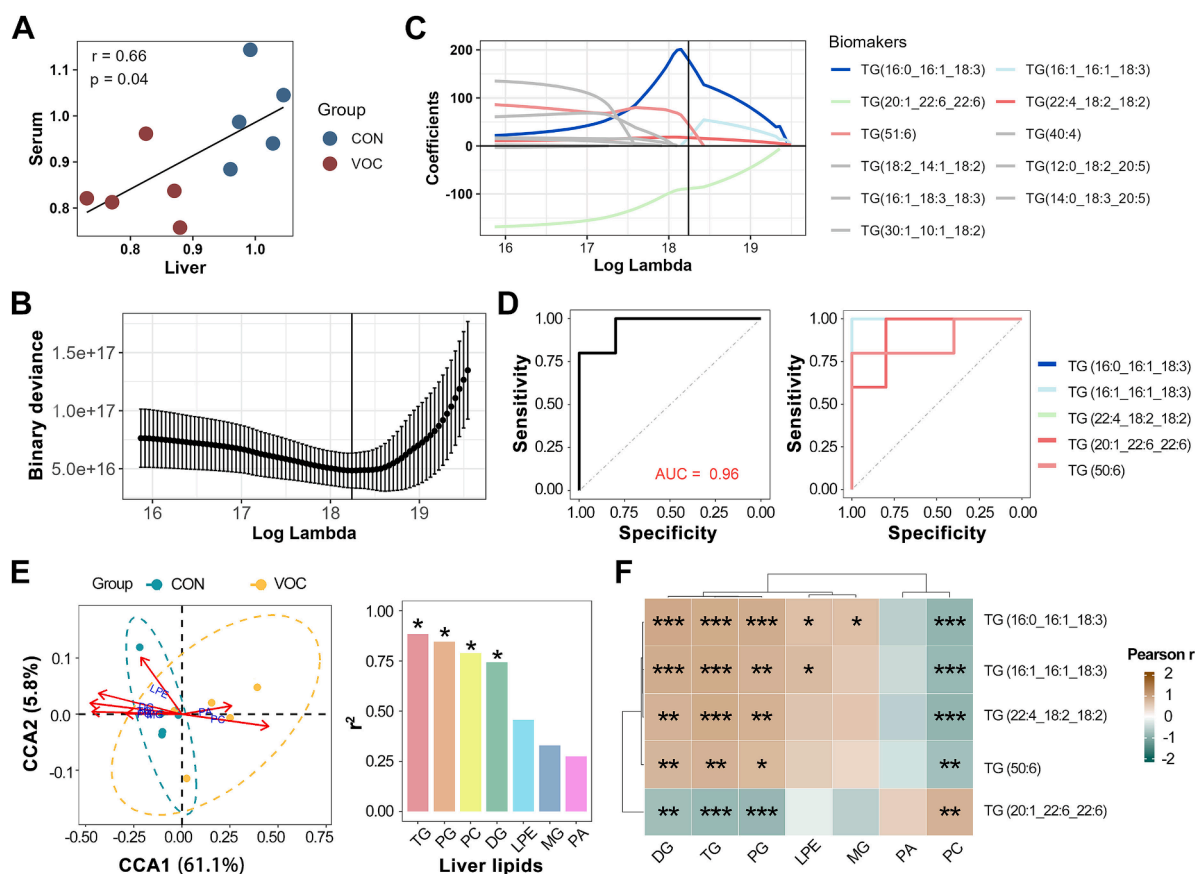


Fig. 3. Serum biomarkers of abnormal hepatic lipids under VOC exposure. (A) Pearson correlation between TG levels in the liver and TG levels in the serum of 10 mice in the CON and VOC groups. (B) The choice of tuning parameter (λ) in the lasso model using tenfold cross-validation based on the minimum criterion. (C) Variation of the coefficients for five markers with the penalty parameter (λ). (D) The ROC plot for the evaluation of 5 lipids biomarkers performance in distinguishing between the CON and VOC groups. (E) CCA plots of lipid biomarkers and classes of lipids mostly altered on the liver from CON and VOC groups, and the correlation analysis. (F) Correlation heat map demonstrating the correlation between five serum lipid biomarkers and several lipid classes affected by VOC in the liver. * indicates Pearson's $p < 0.05$, ** indicates Pearson's $p < 0.01$, *** indicates Pearson's $p < 0.001$.

the decreased expressions of *Aldh3a2*, *Gpat4*, *Gpd2*, *Mogat1*, *Pisd*, *Gpcpd1*, and *Plaat3*, along with the elevated expressions of *Pcyt2*, *Pnpla6*, *Dgkq*, *Akr1b10*, and *Etnppl* (Fig. 4D). Furthermore, TG, DG and MG in the glycerolipid metabolic pathway were all significantly reduced (Fig. 4E), suggesting that the reduction of TG may be related to the reduction of the precursor substance DG. In addition, in the metabolic pathway of glycerophospholipids, PG and LPE were significantly reduced, but PA and PC were significantly increased, indicating that the reduction of DG was related to the interconversion with glycerophospholipids.

Considering that *Dgkq*, a key gene for the interconversion of glycerolipid DG and glycerophospholipid PA, was significantly increased after VOC exposure (Fig. 4D and E), we hypothesized that the conversion between DG and PA was responsible for the significant changes in TG. To test this hypothesis, a correlation analysis of *Dgkq* abundance and the ratio of its mediated metabolites to precursors was performed, and the results showed that *Dgkq* was strong associated with the ratio of upstream DG and downstream PA (fold change = 2.31, $p < 0.01$) (Fig. 4F). Further analysis showed that *Dgkq* was correlated with the changes of PA and DG and their respective metabolic mechanisms, especially with PA, DG, TG and TG/DG (Fig. S11). The data indicated that *Dgkq* may be crucial regulator for the metabolic dysfunction between DG and PA, involved in the decrease of liver TG content.

3.4. Further analysis for crucial mechanism of TG reduction in liver under VOC exposure

To further investigate the in-depth mechanisms of hepatic lipid disorder caused by indoor relevant VOC exposure, paired differential expression analysis was performed, and the results showed that 379 up-regulated and 512 down-regulated DEGs occurred in the VOC group (Fig. 5A). KEGG analysis revealed that the upregulated DEGs were mainly associated with liver injury pathways, such as FoxO signaling pathway and cell cycle, while the downregulated DEGs were mainly associated with fatty acid synthesis and degradation (Fig. 5B). To further determine the potential connections among the pathways, network enrichment analysis of the KEGG pathway showed the FoxO signaling pathway was located in a pivotal position and had strong connections with other pathways (Fig. 5C). Meanwhile, the Forkhead family, to which FoxO transcription factors belong, was significantly enriched in the liver transcriptomic after 8 W of VOC exposure (Fig. S12). These results suggested that FoxO transcription factors and FoxO signaling pathway play a broad regulatory role in the liver upon 8 W of VOC exposure.

Given *Dgkq* tightly correlated with decreased TG after VOC exposure, we aimed to investigate whether FoxO signaling pathway regulate the decrease of TG associated with the *Dgkq*. Initially, we screened 80 lipids and 92 genes closely associated with *Dgkq* in the liver ($|\text{Pearson } r| > 0.9$, $p < 0.05$) and ascertained a high degree of autocorrelation between the lipids and genes, suggesting possible co-expression after VOC exposure (Fig. 5D and E). Considering that co-expression modules is

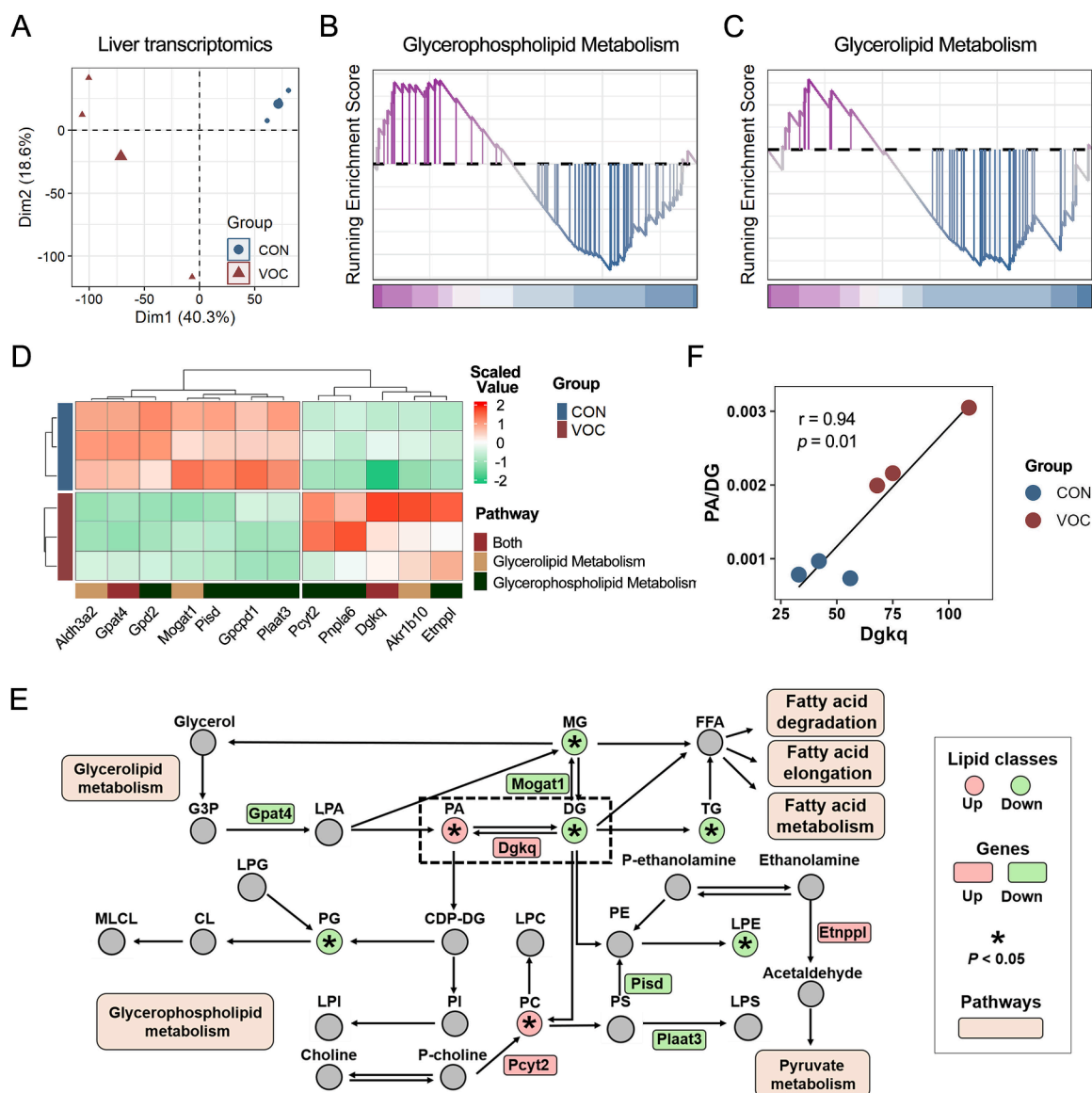


Fig. 4. Potential mechanisms of alterations in the hepatic glycerides and glycerolipids metabolism by 8 W of VOC exposure. (A) Principal component analysis of subjects in the CON and VOC groups. GSEA plot for (B) glycerophospholipid and (C) glycerolipid pathways. (D) Relative expression of genes involved in the glycerophospholipid and glycerolipid pathways in RNA-seq. (E) Selected glycerolipid and glycerophospholipid metabolic reactions from KEGG, with indications of quantified lipid classes (circles) and genes (rectangles) significantly regulated in VOC group. (F) The ratio of *Dgkq* gene to its downstream lipids and upstream lipids.

capable of clarifying the specific mechanism through omics changes, we applied the dual-omics KEGG to further investigate this potential co-expression. As shown in Fig. 5F, the FoxO pathway was significantly enriched in the co-expression module of *Dgkq*, indicating that the FoxO signaling pathway is closely related to *Dgkq*, along with other metabolic and liver injury pathways. Further correlation analysis in Fig. 5G verified the regulatory role between FoxO transcription factor and *Dgkq*. Foxo1 and Foxo4, the target genes of FoxO transcription factor, showed a notable negative correlation with *Dgkq*, indicating that FoxO transcription factor may negatively regulate *Dgkq* through the two target genes, further promote the expression of *Dgkq* and thus led to the decrease of TG. In addition, DEGs in the FoxO signaling pathway associated with protein hydrolysis or cell cycle (*Skp2*, *G6pc*, *Ccnb2* and *Cdkn1a*) were also remarkably correlated with *Dgkq*. The changes in these key mechanistic genes were further verified by qPCR analysis of liver tissue. As demonstrated in Fig. 5H, *Dgkq* expression was upregulated and FoxO transcription factor target genes (*Foxo1* and *Foxo4*) expressions were downregulated under VOC exposure ($p < 0.05$).

Meanwhile, immunofluorescence showed a significant increase in the expression of DGKQ in the liver (Fig. 5I) and a significant decrease in the expression of FOXO1 in the nucleus of hepatocyte (Fig. 5J) upon VOC exposure, which was consistent with the result of transcriptomics and PCR. These findings suggested that *Dgkq* is regulated by FoxO transcription factors, leading to a decrease in TG.

In addition, the results in Fig. 5B suggested that 8 W of VOC exposure resulted in significant downregulation of pathways related to fatty acid synthesis and degradation. GSEA analysis showed downregulation of fatty acid synthesis pathways, indicating reduced liver fatty acid content (Fig. S13). Significant reductions in longer fatty acyl chains were observed under VOC exposure, while short chains remained unchanged (Fig. S14). TG with different carbon numbers or double bond content also decreased. The results revealed that the inability of fatty acid chain synthesis to fill the depletion of degradation can also be a potential reason for the decrease of TG. In order to further explore the potential mechanisms at the metabolic level, changes in metabolic pathways were analyzed using dual omics KEGG. The co-expression of *Dgkq* and FOXO

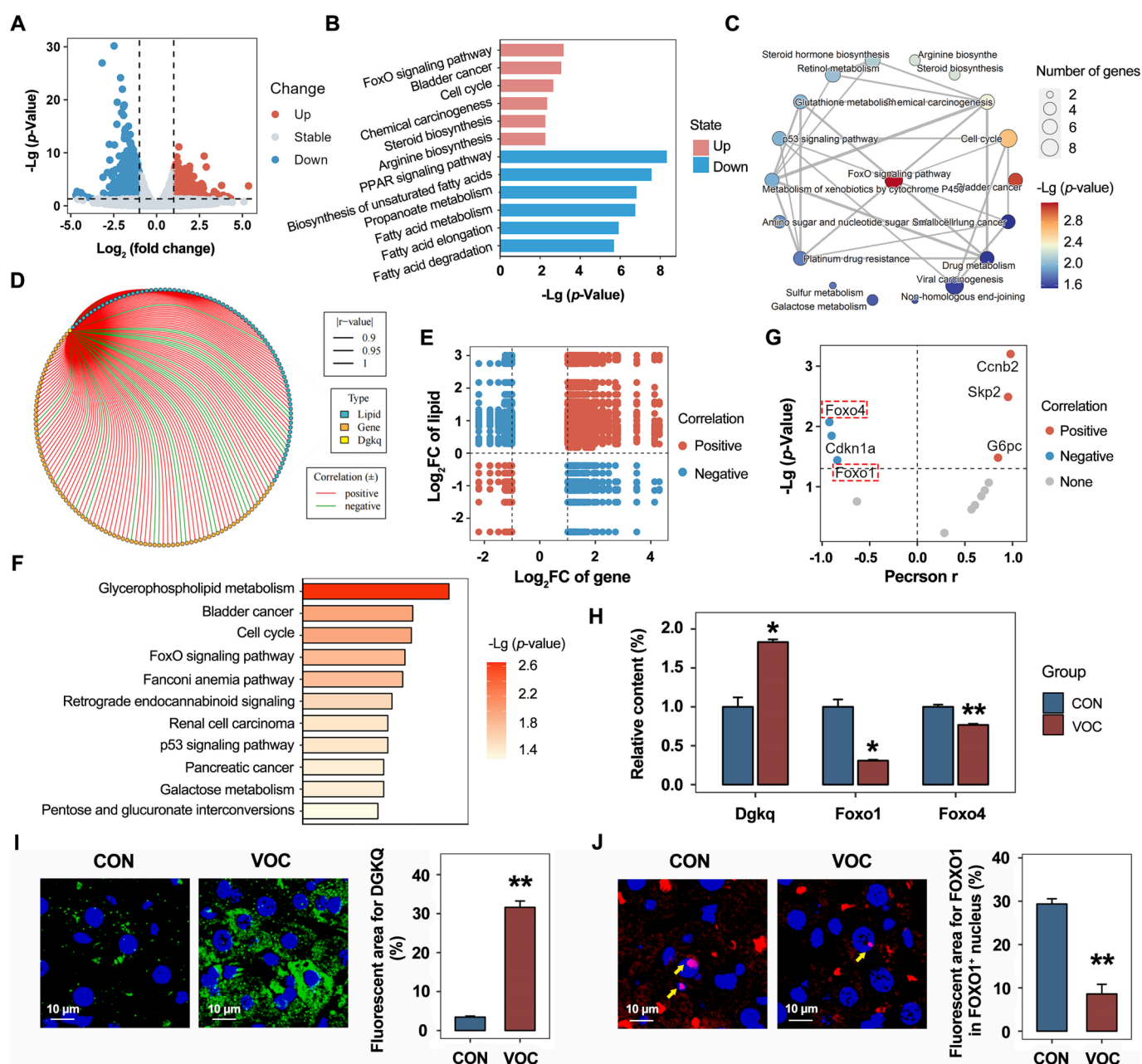


Fig. 5. Upstream mechanisms of hepatic lipid disorders caused by VOC exposure using multi-omics analysis. (A) Volcano plots of the CON and VOC groups comparing ploidy changes and p values of individual genes. (B) KEGG analysis of up-regulated DEGs and down-regulated DEGs between the CON and VOC groups. (C) Pathway enrichment network diagram for up-regulated DEGs. (D) Correlation network to screen DLs and DEGs in the liver strongly correlated with *Dgkq* ($|$ Pearson $r| > 0.9$, $p < 0.05$). (E) Six-quadrant plot of the lipids and genes, with each point representing a strong correlation between each gene and each lipid. (F) KEGG analysis of dual-omics based on genes and lipids strongly associated with *Dgkq*. (G) Scatter plots of FoxO pathway regulated genes or DEGs showing Pearson correlation coefficients and p values for correlation analysis of each gene with *Dgkq*. (H) Expressions of *Dgkq*, *Foxo1* and *Foxo4* in liver. (I) Representative images and quantitative analysis of DGKQ level in liver tissue using immunofluorescence assay. DGKQ (green), nucleus (blue). (J) Representative images and quantitative analysis of FOXO1 level in nucleus of hepatocyte using immunofluorescence assay. FOXO1 (red), nucleus (blue). Scale bar = 10 μm . Data were expressed as mean \pm SEM ($n = 3$). * $p < 0.05$, ** $p < 0.01$, versus the respective CON group. Data were expressed as mean \pm SEM ($n = 3$). * $p < 0.05$, ** $p < 0.01$, versus the respective CON group.

transcription factors had the same enrichment as the overall significant pathway in the liver, and there was also a correlation with related significant genes (Fig. S15). This finding suggested that indoor relevant VOC exposure regulated *Dgkq* through FOXO transcription factors, which in turn affected the synthesis and decomposition of lipids and fatty acids. This dysregulation of lipid metabolism led to lipid disorders, accompanied by energy metabolism disorders, resulting in a decrease in the detoxification ability of the liver and ultimately leading to liver toxicity damage.

4. Discussion

Indoor air pollution exhibited increasingly significant public health concern, in which VOC represented the relatively majority (Cohen et al., 2017). Previous study demonstrated that the specific adverse consequences of liver injury induced by VOC are worthy of further study, especially in the case of liver lipid metabolism disorder, which can be reflected by the changes in serum lipids (Konieczna et al., 2014). Thus, serum lipid indicators are effective biomarkers used to assess liver

health. This study, for the first time, elaborated the liver lipid injury characteristic, identified more serum lipid indicators, and clarified the potential mechanism of liver adverse outcome stimulated by the indoor relevant VOC. We found that VOC caused hepatic lipid disorder and damaged liver fat accumulation. TG (16:0_16:1_18:3), TG (16:1_16:1_18:3), TG (20:1_22:6_22:6), TG (22:4_18:2_18:2) and TG (51:6) in serum lipid were filtered as biomarkers to elaborate the hepatic lipid disorders induced by VOC, using the dual-omics analysis and machine learning. In addition, dual-omics analysis revealed that *Dgkq* was a key target of hepatic lipid disorders and negatively regulated by FoxO transcription factors. Our study helps to understand the characteristics and biomarkers of liver damage caused by VOC exposure, and provides unparalleled potential support to prevent or mitigate the harmful effects of VOC pollutant.

Previous study only investigated the characteristic of liver damage induced by VOC using individual or a few components, which could not reflect the main alteration by VOC exposure in the real environment. For instance, Wang investigated that VOC mixture (formaldehyde, benzene, toluene, and xylene) exposure contributed to significant DNA damage and oxidative damage in liver (Wang et al., 2013). In this study, an indoor relevant VOC exposure model was utilized to simulate real-life exposure scenarios. The complexity of air composition highlights the importance of using this exposure model, which can accurately isolate the effects of VOC exposure from other air components, highlighting its practicability in exploring the health effects of VOC exposure. Using the whole-body inhaled VOC mouse exposure model, our results indicated a decrease of overall liver fat accumulation, which may result from the disorder of hepatic lipid metabolism induced by VOC exposure, thereby reducing lipid biosynthesis and fatty acid biosynthesis. The variation of liver lipid composition disordered the coordination of fatty acid uptake, synthesis, oxidative decomposition, lipid export, and redistribution in the liver, which resulted in multiple liver disease (Fang et al., 2022). In our study, TG and precursor DG, as well as MG and PG were significantly reduced in the liver, while PA, PC, MGDG and SM were increased caused by VOC exposure, indicating the disturbances of lipid metabolism. The decrease in TG and DG observed in lipid composition imply that an inadequate energy supply and a diminished metabolic function of the liver, while an increase in PA may also contribute to liver inflammation and fibrosis risk (Saito et al., 2015; Siddiqui et al., 2015). In this study, aldehydes, ketones, aromatics, alkenes and alkynes accounted for approximately 44 % of the total VOC composition. Previous studies have shown that high concentrations of acetone may trigger liver injury associated with lipid disorders and oxidative stress (Zhang et al., 2018). The toxicity of vinyl chloride and perchloroethylene significantly alter lipid homeostasis in the liver, and there is evidence that perchloroethylene may act through the PPAR α pathway (Anders et al., 2016; Zhou et al., 2017). Acrolein triggers lipid peroxidation adducts leading to oxidative stress and inflammation (Moghe et al., 2015), which is similar to the effects of mixed exposure to VOC components such as toluene (Moro et al., 2010). Recent studies suggest that VOCs and their metabolites may interfere with metabolism and signaling, affecting lipid homeostasis and depleting hepatic energy reserves (Lang and Beier, 2018).

Alteration in serum lipids can indicate the disturbances of hepatic lipids metabolism. Salehpour founded long-term VOC exposure impaired serum lipid in biochemical workers using the kits (Salehpour et al., 2019). However, the serum lipid biomarkers reflecting the alteration of hepatic lipid metabolism profiles are still unclear. Our results showed a close relationship between serum lipids and hepatic lipids, as evidenced by a significant correlation between serum TG levels and liver TG levels. Moreover, it was determined that TG (16:0_16:1_18:3), TG (16:1_16:1_18:3), TG (20:1_22:6_22:6), TG (22:4_18:2_18:2), and TG (51:6) were able to distinguish VOC and control groups with high specificity and showed high accuracy for hepatic lipid disturbances dominated by TG decline. These TGs are all long-chain TGs, which are the main form of energy storage in fat cells, and their metabolism in the body is closely related to serum lipid levels and liver health (Keller and

Layer, 2014; Nosaka et al., 2022). In previous studies, eight long-chain TGs were also found in serum as biomarkers related to hepatic steatosis (Draijer et al., 2020). Notably, we used LASSO regression for biomarker screening, which has the advantage of coping with strong feature selection on high-dimensional data, being able to handle high-dimensional data and covariance data, as well as having better model interpretation compared to traditional regression models (Yin et al., 2022).

As a comprehensive and high-throughput biological research method, various omics have been widely used to appraise the health hazard of environmental pollutants (Tang et al., 2022). In this study, transcriptomic revealed downregulation of glycerolipid and glycerophospholipid metabolism pathways, which contributed to the decreasing of liver TG (Yang et al., 2022). Using multi-omics approaches, this study determined the key gene *Dgkq* for lowering TG levels after screening by correlation analysis. In previous studies, *Dgkq* has been associated with a variety of pathological states, including Parkinson's disease, asthma, and dry syndrome (Lessard et al., 2013; Nalls et al., 2014; Vermeulen et al., 2020). In the liver, the *Dgkq* gene encodes an enzyme, diglyceride kinase, that converts DG to PA, thereby regulating the levels of DG and PA in the liver, and causing some homeostasis disequilibrium (Fernandes et al., 2023; Zheng et al., 2023).

In addition, this study identified the importance of the FoxO transcription factors in the regulation of VOC-induced disorders of hepatic lipid metabolism. In previous studies, hepatic FoxO transcription factors have been shown to regulate lipid metabolism in the liver, which resulted in the liver accumulation in the same direction (Kim et al., 2021). Foxo1 activity promotes hypertriglyceridemia, and Foxo1/3/4 deficiency triggers a marked increase in the expression of inflammatory and fibrotic genes (Pan et al., 2017; Tikhanovich et al., 2013). This study reached a consistent conclusion that the downregulation of FoxO transcription factors was accompanied by liver inflammation and the reduction of hepatic and serum lipids. DEGs in the FoxO signaling pathway associated with protein hydrolysis or cell cycle were also found to be significantly associated with *Dgkq*, such as *Skp2*, *G6pc*, *Ccnb2* and *Cdkn1a*. Previous study reported that *Skp2* played an important role in cell proliferation, differentiation and migration, *G6pc* was involved in hepatic gluconeogenesis and glycogenolysis, and that *Ccnb2* and *Cdkn1a* were involved in the regulating of cell cycle (Gao et al., 2022; Liu et al., 2009; Youns and Abdel Halim Hegazy, 2017). These genes were significantly associated with *Dgkq* and might play a regulatory role in VOC-induced disorders of hepatic lipid metabolism. Hence, this study revealed that VOC exposure caused an increase in Foxo1 and Foxo4, leading to a decrease in *Dgkq* expression, which ultimately induced hepatic lipid disorders and liver injury. Nevertheless, the further *in vitro* study is needed to elucidate the underlying mechanisms for the results obtained in this research.

5. Conclusion

Using an indoor relevant VOC exposure model and multi-omics approaches, including liver lipidomic, serum lipidomic, and liver transcriptomic, this study comprehensively investigated the adverse characteristics of VOC on hepatic lipid metabolism and liver damage. Lipidomic analysis revealed that indoor relevant VOC exposure could lead to lipid metabolism disorder in the liver, characterized by the decrease of TG and its precursor DG. Through machine learning, we identified five serum lipid biomarkers, which can effectively reflected the hepatic lipid disorders induced by VOC. Additionally, multi-omics analysis revealed that the upregulation of *Dgkq* disrupted the interconversion of DG and PA, leading to TG downregulation. Notably, the downregulation of the FoxO transcription factor by VOC contributed to the upregulation of *Dgkq*. Overall, our findings provide valuable data for the understanding of indoor VOC-induced liver damage and provide novel insights into the associated mechanisms. These results may have implications for developing interventions to prevent or mitigate the harmful effects of indoor VOC exposure.

CRedit authorship contribution statement

Gan Miao: Conceptualization, Investigation, Methodology, Writing – original draft. **Yu Wang:** Methodology, Formal analysis, Data curation. **Baoqiang Wang:** Methodology, Writing – original draft. **Hongyan Yu:** Validation, Writing – review & editing. **Jing Liu:** Methodology, Validation. **Ruonan Pan:** Visualization, Formal analysis. **Chengying Zhou:** Methodology, Formal analysis. **Jie Ning:** Methodology, Validation. **Yuxin Zheng:** Supervision, Project administration, Funding acquisition. **Rong Zhang:** Methodology, Resources, Writing – review & editing. **Xiaoting Jin:** Supervision, Project administration, Funding acquisition, Writing – review & editing.

Declaration of Competing Interest

The authors declare that they have no known competing financial interests or personal relationships that could have appeared to influence the work reported in this paper.

Data availability

Data will be made available on request.

Acknowledgments

This work was financially supported by the National Natural Science Foundation of China (No. 92043202, 21976114, and 82241086), the Taishan Scholars Program of Shandong Province (No. tsqn201909101), and the Guangdong Provincial Natural Science Foundation Team Project (2018B030312005).

Appendix A. Supplementary material

Supplementary Information Available: details of the measuring method and results for mice body weights and liver coefficient (Fig. S1-S2), the concentration and compositions of VOC (Table S1-S2), sequences of primers used for qPCR analysis (Table S3), supplementary analysis for hepatic lipidomics (Fig. S3-S8), results of HE images in the liver (Fig. S9), content of serum lipids (Fig. S10), information on serum biomarkers (Table S4), correlation verification of key gene (Fig. S11) and supplementary analysis for multi-omics (Fig. S12-S15). Supplementary data to this article can be found online at <https://doi.org/10.1016/j.envint.2023.108221>.

References

- Anders, L.C., Yeo, H., Kaelin, B.R., Lang, A.L., Bushau, A.M., Douglas, A.N., Cave, M., Arteel, G.E., McClain, C.J., Beier, J.I., 2016. Role of dietary fatty acids in liver injury caused by vinyl chloride metabolites in mice. *Toxicol. Appl. Pharmacol.* 311, 34–41. <https://doi.org/10.1016/j.taap.2016.09.026>.
- Carotti, S., Aquilano, K., Valentini, F., Ruggiero, S., Alletto, F., Morini, S., Picardi, A., Antonelli-Incalzi, R., Lettieri-Barbato, D., Vespasiani-Gentilucci, U., 2020. An overview of deregulated lipid metabolism in nonalcoholic fatty liver disease with special focus on lysosomal acid lipase. *Am. J. Physiol. Gastrointest. Liver Physiol.* 319, G469–G480. <https://doi.org/10.1152/ajpgi.00049.2020>.
- Cohen, A.J., Brauer, M., Burnett, R., Anderson, H.R., Frostad, J., Estep, K., Balakrishnan, K., Brunekreef, B., Dandona, L., Dandona, R., Feigin, V., Freedman, G., Hubbell, B., Jobling, A., Kan, H., Knibbs, L., Liu, Y., Martin, R., Morawska, L., Pope 3rd, C.A., Shin, H., Straik, K., Shaddick, G., Thomas, M., van Dingenen, R., van Donkelaar, A., Vos, T., Murray, C.J.L., Forouzanfar, M.H., 2017. Estimates and 25-year trends of the global burden of disease attributable to ambient air pollution: an analysis of data from the Global Burden of Diseases Study 2015. *Lancet* 389, 1907–1918. [https://doi.org/10.1016/S0140-6736\(17\)30505-6](https://doi.org/10.1016/S0140-6736(17)30505-6).
- Da, Z., Gao, L., Su, G., Yao, J., Fu, W., Zhang, J., Zhang, X., Pei, Z., Yue, P., Bai, B., Lin, Y., Meng, W., Li, X., 2020. Bioinformatics combined with quantitative proteomics analyses and identification of potential biomarkers in cholangiocarcinoma. *Cancer Cell Int.* 20, 130. <https://doi.org/10.1186/s12935-020-01212-z>.
- de Mello, V.D., Kolehmanien, M., Schwab, U., Pulkkinen, L., Uusitupa, M., 2012. Gene expression of peripheral blood mononuclear cells as a tool in dietary intervention studies: What do we know so far? *Mol. Nutr. Food Res.* 56, 1160–1172. <https://doi.org/10.1002/mnfr.201100685>.
- Draijer, L.G., Froom-Torenstra, D., van Weeghel, M., Vaz, F.M., Bohte, A.E., Holleboom, A.G., Benninga, M.A., Koot, B.G.P., 2020. Lipidomics in nonalcoholic fatty liver disease: exploring serum lipids as biomarkers for pediatric nonalcoholic fatty liver disease. *J. Pediatr. Gastroenterol. Nutr.* 71, 433–439. <https://doi.org/10.1097/mpg.0000000000002875>.
- Fang, C., Pan, J., Qu, N., Lei, Y., Han, J., Zhang, J., Han, D., 2022. The AMPK pathway in fatty liver disease. *Front. Physiol.* 13, 970292. <https://doi.org/10.3389/fphys.2022.970292>.
- Fernandes, T., Domingues, M.R., Moreira, P.I., Pereira, C.F., 2023. A perspective on the link between mitochondria-associated membranes (MAMs) and lipid droplets metabolism in neurodegenerative diseases. *Biology (Basel)* 12. doi: 10.3390/biology12030414.
- Fuller, R., Landrigan, P.J., Balakrishnan, K., Bathan, G., Bose-O'Reilly, S., Brauer, M., Caravanos, J., Chiles, T., Cohen, A., Corra, L., Cropper, M., Ferraro, G., Hanna, J., Hanrahan, D., Hu, H., Hunter, D., Janata, G., Kupka, R., Lanphear, B., Lichtveld, M., Martin, K., Mustapha, A., Sanchez-Triana, E., Sandilya, K., Schaeffli, L., Shaw, J., Seddon, J., Suk, W., Téllez-Rojo, M.M., Yan, C., 2022. Pollution and health: a progress update. *Lancet Planet Health* 6, e535–e547. [https://doi.org/10.1016/s2542-5196\(22\)00090-0](https://doi.org/10.1016/s2542-5196(22)00090-0).
- Gao, H., Zhou, L., Zhong, Y., Ding, Z., Lin, S., Hou, X., Zhou, X., Shao, J., Yang, F., Zou, X., Cao, H., Xiao, G., 2022. Kindlin-2 haploinsufficiency protects against fatty liver by targeting Foxo1 in mice. *Nat. Commun.* 13, 1025. <https://doi.org/10.1038/s41467-022-28692-z>.
- Keller, J., Layer, P., 2014. The Pathophysiology of Malabsorption. *Viszeralmedizin* 30 (3), 150–154. <https://doi.org/10.1159/000364794>.
- Kim, D.H., Bang, E., Ha, S., Jung, H.J., Choi, Y.J., Yu, B.P., Chung, H.Y., 2021. Organ-differential roles of Akt/FoxOs axis as a key metabolic modulator during aging. *Aging Dis.* 12 (7), 1713–1728. <https://doi.org/10.14336/ad.2021.0225>.
- Konicieczna, J., Sánchez, J., van Schothorst, E.M., Torrens, J.M., Bunschoten, A., Palou, M., Picó, C., Keijer, J., Palou, A., 2014. Identification of early transcriptome-based biomarkers related to lipid metabolism in peripheral blood mononuclear cells of rats nutritionally programmed for improved metabolic health. *Genes Nutr.* 9, 366. <https://doi.org/10.1007/s12263-013-0366-2>.
- Lang, A.L., Beier, J.I., 2018. Interaction of volatile organic compounds and underlying liver disease: a new paradigm for risk. *Biol. Chem.* 399, 1237–1248. <https://doi.org/10.1515/hsz-2017-0324>.
- Lessard, C.J., Li, H.E., Adrianto, I., Ice, J.A., Rasmussen, A., Grundahl, K.M., Kelly, J.A., Dozromov, M.G., Miceli-Richard, C., Bowman, S., Lester, S., Eriksson, P., Eloranta, M.-L., Brun, J.G., Göransson, L.G., Harboe, E., Guthridge, J.M., Kaufman, K.M., Kvarnström, M., Jazebi, H., Graham, D.S.C., Grandits, M.E., Nazmul-Hossain, A.N.M., Patel, K., Adler, A.J., Maier-Moore, J.S., Farris, A.D., Brennan, M. T., Lessard, J.A., Chodosh, J., Gopalakrishnan, R., Hefner, K.S., Houston, G.D., Huang, A.J.W., Hughes, P.J., Lewis, D.M., Radfar, L., Rohrer, M.D., Stone, D.U., Wren, J.D., Vyse, T.J., Gaffney, P.M., James, J.A., Omdal, R., Wahren-Herlenius, M., Illei, G.G., Witte, T., Jonsson, R., Rischmueller, M., Rönnblom, L., Nordmark, G., Ng, W.-F., Mariette, X., Anaya, J.-M., Rhodus, N.L., Segal, B.M., Scofield, R.H., Montgomery, C.G., Harley, J.B., Sivills, K.L., 2013. Variants at multiple loci implicated in both innate and adaptive immune responses are associated with Sjögren's syndrome. *Nat. Genet.* 45 (11), 1284–1292. <https://doi.org/10.1038/ng.2792>.
- Liu, J., Drane, W., Liu, X., Wu, T., 2009. Examination of the relationships between environmental exposures to volatile organic compounds and biochemical liver tests: application of canonical correlation analysis. *Environ. Res.* 109, 193–199. <https://doi.org/10.1016/j.envres.2008.11.002>.
- Moghe, A., Ghare, S., Lamoreau, B., Mohammad, M., Barve, S., McClain, C., Joshi-Barve, S., 2015. Molecular mechanisms of acrolein toxicity: relevance to human disease. Molecular mechanisms of acrolein toxicity: relevance to human disease. *Toxicol. Sci.* 143, 242–255. <https://doi.org/10.1093/toxsci/ktf233>.
- Moro, A.M., Charão, M., Brucker, N., Bulcão, R., Freitas, F., Guerreiro, G., Baierle, M., Nascimento, S., Waechter, F., Hirakata, V., Linden, R., Thiesen, F.V., Garcia, S.C., 2010. Effects of low-level exposure to xenobiotics present in paints on oxidative stress in workers. *Sci. Total Environ.* 408, 4461–4467. <https://doi.org/10.1016/j.scitotenv.2010.06.058>.
- Nalls, M.A., Pankratz, N., Lill, C.M., Do, C.B., Hernandez, D.G., Saad, M., DeStefano, A.L., Kara, E., Bras, J., Sharma, M., Schulte, C., Keller, M.F., Arepalli, S., Letson, C., Edsall, C., Stefansson, H., Liu, X., Pliner, H., Lee, J.H., Cheng, R., Ikram, M.A., Ioannidis, J.P.A., Hadjigeorgiou, G.M., Bis, J.C., Martinez, M., Perlmutter, J.S., Goate, A., Marder, K., Fiske, B., Sutherland, M., Xiromerisiou, G., Myers, R.H., Clark, L.N., Stefansson, K., Hardy, J.A., Heutink, P., Chen, H., Wood, N.W., Houlihan, H., Payami, H., Brice, A., Scott, W.K., Gasser, T., Bertram, L., Eriksson, N., Foroud, T., Singleton, A.B., 2014. Large-scale meta-analysis of genome-wide association data identifies six new risk loci for Parkinson's disease. *Nat. Genet.* 46 (9), 989–993. <https://doi.org/10.1038/ng.3043>.
- Nosaka, N., Tsujino, S., Kato, K., 2022. Short-term ingestion of medium-chain triglycerides could enhance postprandial consumption of ingested fat in individuals with a body mass index from 25 to less than 30: a randomized, placebo-controlled, double-blind crossover study. *Nutrients* 14 (5), 1119. <https://doi.org/10.3390/nu14051119>.
- Pan, X., Zhang, Y., Kim, H.G., Liangpunsakul, S., Dong, X.C., 2017. FOXO transcription factors protect against the diet-induced fatty liver disease. *Sci. Rep.* 7, 44597. <https://doi.org/10.1038/srep44597>.
- Saito, K., Uebanso, T., Maekawa, K., Ishikawa, M., Taguchi, R., Nammo, T., Nishimaki-Mogami, T., Udagawa, H., Fujii, M., Shibasaki, Y., Yoneyama, H., Yasuda, K., Saito, Y., 2015. Characterization of hepatic lipid profiles in a mouse model with nonalcoholic steatohepatitis and subsequent fibrosis. *Sci. Rep.* 5, 12466. <https://doi.org/10.1038/srep12466>.

- Salehpour, S., Amani, R., Nili-Ahmadabadi, A., 2019. Volatile organic compounds as a preventive health challenge in the petrochemical industries. *Int. J. Prev. Med.* 10, 194. https://doi.org/10.4103/ijpvm.IJPVM.495_18.
- Shuai, J., Kim, S., Ryu, H., Park, J., Lee, C.K., Kim, G.B., Ultra Jr., V.U., Yang, W., 2018. Health risk assessment of volatile organic compounds exposure near daegu dyeing industrial complex in South Korea. *BMC Public Health* 18, 528. <https://doi.org/10.1186/s12889-018-5454-1>.
- Siddiqui, R.A., Xu, Z., Harvey, K.A., Pavlina, T.M., Becker, M.J., Zaloga, G.P., 2015. Comparative study of the modulation of fructose/sucrose-induced hepatic steatosis by mixed lipid formulations varying in unsaturated fatty acid content. *Nutr. Metab. (Lond.)* 12, 41. <https://doi.org/10.1186/s12986-015-0038-x>.
- Stange, J., Mitzner, S.R., Klammt, S., Freytag, J., Peszynski, P., Loock, J., Hickstein, H., Korten, G., Schmidt, R., Hentschel, J., Schulz, M., Löhr, M., Liebe, S., Schareck, W., Hopt, U.T., 2000. Liver support by extracorporeal blood purification: a clinical observation. *Liver Transpl.* 6, 603–613. <https://doi.org/10.1053/jlts.2000.7576>.
- Tang, S., Xie, J., Fang, W., Wen, X., Yin, C., Meng, Q., Zhong, R., Chen, L., Zhang, H., 2022. Chronic heat stress induces the disorder of gut transport and immune function associated with endoplasmic reticulum stress in growing pigs. *Anim. Nutr.* 11, 228–241. <https://doi.org/10.1016/j.aninu.2022.08.008>.
- Tikhanovich, I., Cox, J., Weinman, S.A., 2013. Forkhead box class O transcription factors in liver function and disease. *J. Gastroenterol. Hepatol.* 28 (Suppl. 1), 125–131. <https://doi.org/10.1111/jgh.12021>.
- Vermeulen, C.J., Xu, C.-J., Vonk, J.M., ten Hacken, N.H.T., Timens, W., Heijink, I.H., Nawijn, M.C., Boekhoudt, J., van Oosterhout, A.J., Affleck, K., Weckmann, M., Koppelman, G.H., van den Berge, M., 2020. Differential DNA methylation in bronchial biopsies between persistent asthma and asthma in remission. *Eur. Respir. J.* 55 (2), 1901280. <https://doi.org/10.1183/13993003.01280-2019>.
- Villeneuve, P.J., Jerrett, M., Su, J., Burnett, R.T., Chen, H., Brook, J., Wheeler, A.J., Cakmak, S., Goldberg, M.S., 2013. A cohort study of intra-urban variations in volatile organic compounds and mortality, Toronto, Canada. *Environ. Pollut.* 183, 30–39. <https://doi.org/10.1016/j.envpol.2012.12.022>.
- Wallace, M.A., Kormos, T.M., Pleil, J.D., 2016. Blood-borne biomarkers and bioindicators for linking exposure to health effects in environmental health science. *J. Toxicol. Environ. Health B Crit. Rev.* 19, 380–409. <https://doi.org/10.1080/10937404.2016.1215772>.
- Wang, F., Li, C., Liu, W., Jin, Y., 2013. Oxidative damage and genotoxic effect in mice caused by sub-chronic exposure to low-dose volatile organic compounds. *Inhal. Toxicol.* 25, 235–242. <https://doi.org/10.3109/08958378.2013.779767>.
- Wang, T., Shao, W., Huang, Z., Tang, H., Zhang, J., Ding, Z., Huang, K., 2021. MOGONET integrates multi-omics data using graph convolutional networks allowing patient classification and biomarker identification. *Nat. Commun.* 12, 3445. <https://doi.org/10.1038/s41467-021-23774-w>.
- Yang, Y., Yang, S., Tang, J., Ren, G., Shen, J., Huang, B., Lei, C., Chen, H., Qu, K., 2022. Comparisons of hematological and biochemical profiles in Brahman and Yunling cattle. *Animals (Basel)* 12 (14), 1813. <https://doi.org/10.3390/ani12141813>.
- Yin, T., Shi, S., Zhu, X., Cheang, I., Lu, X., Gao, R., Zhang, H., Yao, W., Zhou, Y., Li, X., 2022. A survival prediction for acute heart failure patients via web-based dynamic nomogram with internal validation: a prospective cohort study. *J. Inflamm. Res.* 15, 1953–1967. <https://doi.org/10.2147/jir.S348139>.
- Youns, M., Abdel Halim Hegazy, W., 2017. The natural flavonoid fisetin inhibits cellular proliferation of hepatic, colorectal, and pancreatic cancer cells through modulation of multiple signaling pathways. *PLoS One* 12, e0169335. <https://doi.org/10.1371/journal.pone.0169335>.
- Yu, Y.M., Zhou, B.H., Yang, Y.L., Guo, C.X., Zhao, J., Wang, H.W., 2022. Estrogen deficiency aggravates fluoride-induced liver damage and lipid metabolism disorder in rats. *Biol. Trace Elem. Res.* 200 (6), 2767–2776. <https://doi.org/10.1007/s12011-021-02857-1>.
- Zhang, R., Wang, Y., Zhang, Z., Cao, J., 2018. Highly sensitive acetone gas sensor based on g-C₃N₄ decorated MgFe₂O₄ porous microspheres composites. *Sensors* 18, 2211. <https://doi.org/10.3390/s18072211>.
- Zhang, J., Zhou, Q., Su, R., Sun, Z., Zhang, W., Jin, X., Zheng, Y., 2020. Cardiac dysfunction and metabolic remodeling due to seasonally ambient fine particles exposure. *Sci. Total Environ.* 721, 137792. <https://doi.org/10.1016/j.scitotenv.2020.137792>.
- Zheng, J., Pang, Y., Zhang, Y., Hu, W., Yang, P., Liu, Q., Ning, J., Du, Z., Jin, X., Tang, J., Niu, Y., Zheng, Y., Zhang, R., 2022. Indoor VOCs exposure induced Parkinson-like behaviors through autophagy dysfunction and NLRP3 inflammasome-mediated neuroinflammation. *J. Hazard. Mater.* 440, 129818. <https://doi.org/10.1016/j.jhazmat.2022.129818>.
- Zheng, Z.G., Xu, Y.Y., Liu, W.P., Zhang, Y., Zhang, C., Liu, H.L., Zhang, X.Y., Liu, R.Z., Zhang, Y.P., Shi, M.Y., Yang, H., Li, P., 2023. Discovery of a potent allosteric activator of DGKQ that ameliorates obesity-induced insulin resistance via the sn-1,2-DAG-PKCε signaling axis. *Cell Metab.* 35, 101–117.e111. <https://doi.org/10.1016/j.cmet.2022.11.012>.
- Zhou, Y.H., Cichocki, J.A., Soldatow, V.Y., Scholl, E.H., Gallins, P.J., Jima, D., Yoo, H., Chiu, W., Wright, F., Rusyn, I., 2017. Comparative dose-response analysis of liver and kidney transcriptomic effects of Trichloroethylene and Tetrachloroethylene in B6C3F1 mouse. *Toxicol. Sci.* 160, 95–110. <https://doi.org/10.1093/toxsci/kfx165>.